

# DEVELOPMENT OF MATERIAL OPTIMIZATION TECHNOLOGY FOR INNOVATION

IKUO TANABE & PAULO DA SILVA

Department of Mechanical Engineering, Nagaoka University of Technology, Japan

## ABSTRACT

In recent years, the demand for products of high quality, with hybrid properties, multifunctional, low cost and which is environmentally-friendly has been rapidly increasing. Here, several optimization technologies are currently being used to address these issues. Particularly, topology optimization technology is considered useful in the manufacturing field due to the high quality, high reliability and safety that it offers. However, it has been observed that there is a lack of proper material optimization techniques in the technology development process. There are hundreds of materials used in the industrial field but, surprisingly, there is a minimal amount of research regarding material property optimization for innovative developments. Thus, the present research, through a previously developed software, defined a material optimization technology for innovation. This technology relied on a software that creates new materials with hybrid properties, a hybrid materials manufacturing method, and an algorithm for material optimization. The material optimization technology was then evaluated. It is concluded from the results that: (1) the expanded proposed software was suitable for calculating the Young's modulus, density, coefficient of linear expansion, specific heat and thermal conductivity for several properties; and (2) the material optimization technology was effective for the development of innovative products with defined functions or properties.

*Keywords: material optimization, new material, hybrid property, three-dimensional and functionally gradient material.*

## 1 INTRODUCTION

In the 21st century, the demand for products with high quality [1], hybrid properties [2], multifunctionality [3], low cost and considerable environmental-friendliness [4] has been rapidly increasing. Here, several optimization technologies are currently being used to address these issues. Particularly, topology optimization technology is considered as useful in the manufacturing field due to the high quality, high reliability and safety that it offers. However, it has been observed that there is a lack of proper material optimization techniques in the technology development process. There are hundreds of materials used in the industrial field but, surprisingly, there is a minimal amount of research regarding material property optimization for innovative developments.

Thus, the present research, through a previously developed software, defined a material optimization technology for innovation. This technology relied on a software that creates new materials with hybrid properties, a hybrid materials manufacturing method, and an algorithm for material optimization. The aforementioned software can effectively calculate up to five desired material properties that requested at once (i.e. Young's modulus, density, coefficient of linear expansion, specific heat and thermal conductivity). In addition, the algorithm for material optimization was defined through FEM inverse analysis. The material optimization technology was then evaluated with a simple experiment. In this regard, it was thought that material optimization technologies were highly relevant to explore due to the design and manufacturing implications of having a customized material.



## 2 PROPERTIES CALCULATION MODELS FOR NEW COMPOSITE MATERIALS

In this section a review of a previously developed software and the equations used in it is presented and explained [5]. For this, the following suffixes refer to the following: “s” stands for fine aggregate, “g” for rough aggregate, “e” for bond (e.g. epoxy resin), “a” for air and “c” for concrete or mortar; “t” for continuous layer and “d” for non-continuous layer.

The following model-describing equations [5] were meant for the calculation of the Young’s modulus, density, coefficient of linear expansion and specific heat. In the case of thermal conductivity calculations, the Russell model was used [6]. Every material combination in the developed software for this specific case was constrained to be concrete, porous material and sintered compact. Here, the volume percentage was firstly obtained through eqn (1)

$$\left. \begin{aligned} V_s &= W_s \cdot \rho_c / \rho_s \\ V_g &= W_g \cdot \rho_c / \rho_g \\ V_e &= W_e \cdot \rho_c / \rho_e \\ V_a &= 100 - (V_s + V_g + V_e) \end{aligned} \right\} \quad (1)$$

where  $V$  was volume percentage (%),  $W$  was weight percentage (%),  $\rho$  was density ( $\text{kg/m}^3$ ), and in the case of the porous material or the sintered compact ( $W_e = 0$ ), values of  $V_e = W_e = 10^{-6}$  were used for regular calculation.

As mentioned, the thermal conductivity calculation was done through the Russell model [6] and shown in eqn (2)

$$\lambda_c = \lambda_t \frac{K \cdot V_d^{2/3} + (1 - V_d^{2/3})}{K \cdot (V_d^{2/3} - V_d) + (1 - V_d^{2/3} + V_d)} \quad (2)$$

where  $\lambda$  was thermal conductivity [ $\text{W}/(\text{m/K})$ ] and  $K$  was  $\lambda_d / \lambda_c$ .

In Fig. 1, the calculation models meant for concrete or composite materials are depicted. First, the thermal conductivity calculation for mortar 1 was done (i.e. when the continuous layer was a bonding material and the non-continuous layer was fine aggregate). Subsequently, the second thermal conductivity calculation meant for mortar 2 was done (i.e. when the continuous layer was the mortar 1 and the non-continuous layer was a middle aggregate). Accordingly, the final thermal conductivity calculation was done in the case in which the continuous layer was mortar 2 and the non-continuous layer was a coarse aggregate. For porous or sintered compact materials ( $W_e=0$ ), values of  $V_e = W_e = 10^{-6}$  were utilized.

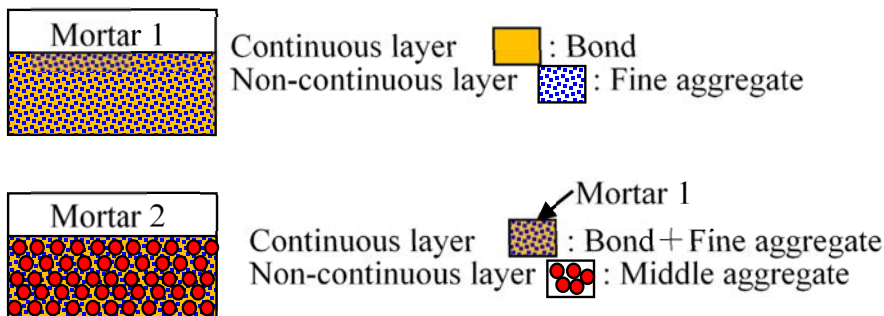


Figure 1: Models for calculation of thermal conductivity.

In addition, the specific heat calculation was done through eqn (3) [5], [7].

$$C_c = [W_s \cdot C_s + W_g \cdot C_g + W_e \cdot C_e + \{(100 - (W_s + W_g + W_e)) \cdot C_a\}] / 100, \quad (3)$$

where  $C$  was specific heat [kJ/(kgK)] and  $W$  was weight percentage [%]. For porous or sintered compact materials ( $W_e=0$ ), values of  $V_e = W_e = 10^{-6}$  were utilized.

Moreover, the coefficient of linear expansion calculation was done through eqn (4)

$$\alpha_c = \frac{\alpha_d \cdot V_d + \alpha_t \{1 + (Y-1) \cdot V_d^{1/3} - Y \cdot V_d\}}{1 + (Y-1) (V_d^{1/3} - V_d)} \quad (4)$$

where  $\alpha$  was linear expansion coeff. [1/K],  $Y$  was  $E_t/E_d$  and  $E$  was Young's modulus (GPa).

Furthermore, the linear expansion coefficient calculations were started with calculations for mortar 1 (i.e. when the continuous layer was a bonding material and the non-continuous layer was fine aggregate). Then, the calculations meant for mortar 2 were done (i.e. when the continuous layer was the mortar 1 and the non-continuous layer was a middle aggregate). Accordingly, the final calculation was done in the case in which the continuous layer was mortar 2 and the non-continuous layer was a coarse aggregate. For porous or sintered compact materials ( $W_e=0$ ), values of  $V_e = W_e = 10^{-6}$  were utilized.

Additionally, the Young's modulus calculation was done through eqn (5)

$$E_c = E_t \left\{ 1 + \frac{V_d}{E_d / (E_d - E_t) - V_d^{1/3}} \right\} \quad (5)$$

where  $E$  was the Young's modulus (GPa). In this regard, the Young's modulus calculations began with calculations for mortar 1 (i.e. when the continuous layer was a bonding material and the non-continuous layer was fine aggregate). After this, the calculations meant for mortar 2 were done (i.e. when the continuous layer was the mortar 1 and the non-continuous layer was a middle aggregate). Finally, calculations for the case in which the continuous layer was mortar 2 and the non-continuous layer was a coarse aggregate. For porous or sintered compact materials ( $W_e=0$ ), values of  $V_e = W_e = 10^{-6}$  were utilized. Consistently, the above equations were then considered as the basis for the following chapters and this research.

### 3 PROPOSED MANUFACTURING PROCESS FOR THE DESIGNED MATERIALS

In a similar way, previous researches defined the proposed manufacturing method for the designed materials using the aforementioned equations inside a software (which defined two scenarios: (1) Selecting materials and calculating appropriate ratios to achieve intended effects; (2) Calculating the properties generated with these ratios and materials, and said method was also applied in this research. Consequently, a review of the process was deemed as appropriate. For the aforementioned software, a solid body uniformity was assumed for each calculation model but conventional manufacturing of concrete or composites (mixing) yields an heterogeneous mix which in result would be considered as a material defect. Thus, the proposed manufacturing process was meant to achieve high quality by avoiding this issue. The manufacturing procedure is shown in Fig. 2 [8], [9]. Here, a coarse aggregate was firstly put into a mold and filled up to about 60 vl.%. Subsequently, a middle aggregate was poured over the coarse aggregate. After this, hydraulic pressure and vibration were applied over the aggregates to homogenize the mixture. For this, the size of the middle aggregate was restricted to be less than one seventh of the coarse aggregate. Here, the available air given space for the middle aggregate was about 40 vl.% relative to the coarse aggregate. Thus, given that the middle aggregate filled up about 60 vl.% of the total space, 40 vl.% would mean that the

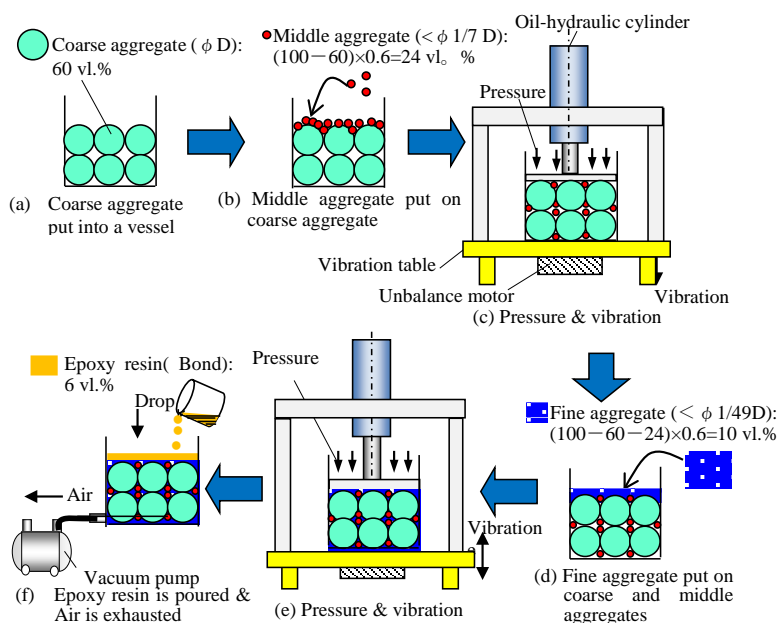


Figure 2: Manufacturing procedure for the composite with hybrid properties.

aggregate filled about 24 vl.% ( $=0.4 \times 0.6$ ). Consequently, the coarse and the middle aggregates uniformly filled up 84 vl.% ( $=60 \text{ vl.}\% + 24 \text{ vl.}\%$ ). In addition, fine aggregate was also poured into the mix to fill the gaps between the middle aggregates. It was thought that this aggregate would have filled up to 10 vl.% ( $= (100-60-24) \times 0.6$ ). As a result, all aggregates uniformly filled around 94 vl.% ( $=60 \text{ vl.}\% + 24 \text{ vl.}\% + 10 \text{ vl.}\%$ ). It must be considered that space was meant to be filled by the aggregates in a rhombic display and, thus, the mixture becomes a mortar structure. Bonding materials (e.g. epoxy resin) were meant to be poured from upper surface over all aggregates, and the air between the aggregates was taken out from the mixture with a vacuum pump located at the bottom of the shown setup. Upon solidification of the bonding materials, the generated composite material was removed from the mold. Here, the component distribution was similar to that of the calculation model.

The calculation accuracy of the material optimization software was evaluated in the mentioned previous researches. The calculations for density, linear expansion coefficient and specific heat were accurate to around  $\pm 5\%$  but the Young's modulus and thermal conductivity were around  $\pm 20\%$ . This was thought to be because of air formation in the composite material and the FEM simulations were modified accordingly; as a result, the software calculation accuracy for the Young's modulus and thermal conductivity reached down to a  $\pm 5\%$  each. This software was then evaluated in several cases with the generation of new composites with hybrid properties [9]–[12].

#### 4 APPLYING THREE-DIMENSIONAL FUNCTIONAL GRADIENT MATERIALS

As an addition to the aforementioned designed materials, considerations regarding a three-dimensional and functionally gradient material, previously developed using the proposed software as an exercise to devise future innovative materials, were thought to be appropriate [12]. The devised manufacturing procedure for this is shown in Fig. 3. The three-dimensional

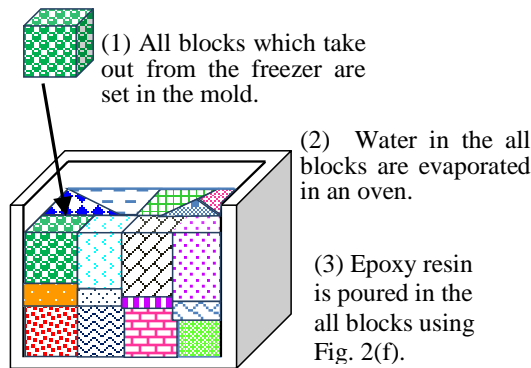


Figure 3: Manufacturing procedure for a three-dimensional and functionally gradient material.

and functionally gradient material was a very complex structure, as each block had several hybrid properties and were arranged in the directions of the X, Y and Z axes. Said hybrid properties were calculated by using the developed software and each block was manufactured using the procedure shown in Fig. 2. However, tap water was utilized in exchange for the bonding material (i.e. epoxy resin) shown in Fig. 2. Here, the blocks were frozen and kept in a freezer. After that, all the blocks were taken out of the freezer and put into a mold, then the frozen tap water in all the blocks was evaporated in an oven. Next, the epoxy resin was poured in exchange for the frozen tap water over all the blocks using Fig. 2(f). The manufactured three-dimensional and functionally gradient material is shown in Fig. 4. Here, the structure was deemed to be unique in the material optimization field.

##### 5 MATERIAL OPTIMIZATION ALGORITHM USING FEM INVERSE ANALYSIS

Nowadays, designers in the manufacturing field rely on computer simulations and CAE systems. Commonly, the input data was the original design, its shape and size, the boundary conditions and several material properties. Here, designers are constrained to the currently available material databases. However, as current technology trends demand ever-increasing



Figure 4: Photograph of a three-dimensional and functionally gradient material.

performances, the need for new materials with improved characteristics is of concern. Therefore, the material optimization technology presented in this paper and in the following chapter consisted in a vertical integration of the previously developed material optimization software, the previously explored manufacturing process and the FEM inverse analysis tools that are explained in this chapter; this was thought to then offer the designers a wider material set of options and improve the quality and performance of their designs.

In this section, an algorithm for material optimization using inverse analysis of the FEM was developed as depicted in Fig. 5. First, the input would be the defined desired functions of the material based on the demanded product characteristics (which could be influenced by marketing data). The most suitable properties to satisfy the desired functions on the innovative product were calculated by both the inverse analysis of the FEM simulation and the method of successive substitution in a personal computer. Here, the FEM simulations were static analysis, thermal analysis and vibration analysis and outlined in Table 1; this table also shows the relationship between the different simulations features and the necessary properties for each analysis. The necessary materials and its composite ratio for the new materials exhibiting the most suitable properties, calculated through the algorithm, were then calculated by the previously developed software [13]. Then the new composite material with the most suitable properties was manufactured using the procedure shown in Section 3. In addition, the innovative product could have the various property distributions by using the three-dimensional functional gradient material manufacturing method shown in Section 4.

## 6 EVALUATION FOR THE MATERIAL OPTIMIZATION TECHNOLOGY

The evaluation of the proposed material optimization technology is covered in this section. The relationship between the desired characteristics and the calculated properties using the algorithm of the material optimization is shown in Table 2. Here, a block with length 60 mm×width 45 mm×height 75 mm was used for the evaluation under two different analyses. The desired block performances (input) were: when the load on the upper surface of the block is 1000 N, the displacement in the vertical direction becomes -3.2  $\mu\text{m}$ ; and resonance

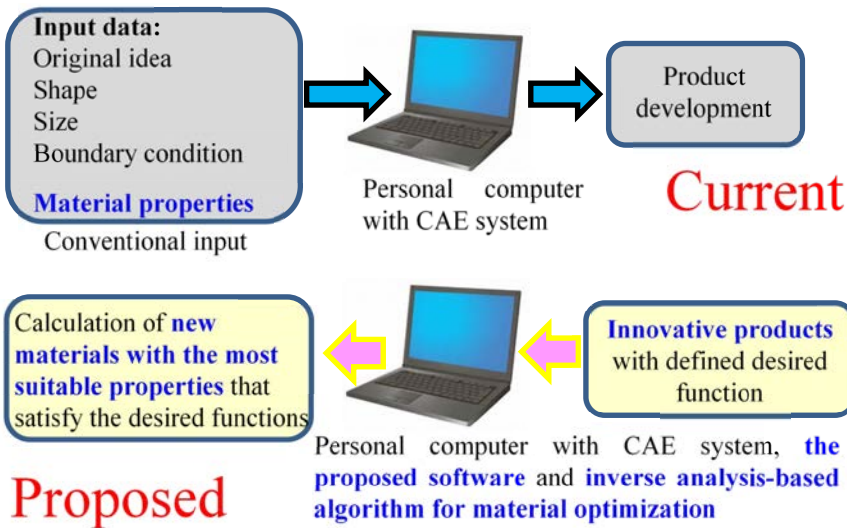


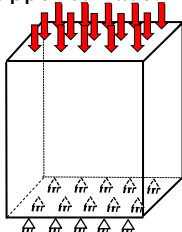
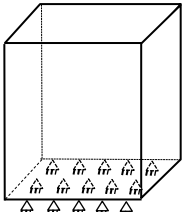
Figure 5: Innovative development using the proposed software and the algorithm for material optimization using FEM inverse analysis.


Table 1: Several properties used for the input data in certain FEM simulations.

Kinds of FEM simulation		Boundary conditions	Input data for FEM
Static analysis		Fix condition	Shape & Size Material properties (Young's modulus & Poisson's ratio)
Thermal analysis	Steady state	Heat transfer coefficient	Shape & Size Material properties (Thermal conductivity)
	Non-steady state	Heat transfer coefficient	Shape & Size Material properties (Density, specific heat and thermal conductivity)
Vibration analysis	Free vibration	Fix condition	Shape & Size Material properties (Young's modulus & density)
	Forced vibration	Fix condition and damping ratio	Shape & Size Material properties (Young's modulus & density)

Note: At thermal deformation analysis, both Static and Thermal analysis are used, and coefficient of linear expansion is also used for input data. Poisson's ratio is always 0.3.

Table 2: Relationship between the desired characteristics and the calculated properties using the algorithm of the material optimization.

The desired characteristics for the block with 60 mm×45 mm×75 mm.	The displacement in the height direction become -3.2 $\mu\text{m}$ at 1000 N load.
	The resonance frequencies of the first and the second models are 5200 Hz and 6100 Hz respectively.
<p>The FEM models for the inverse analysis</p> <div style="display: flex; justify-content: space-around; align-items: flex-start;"> <div style="text-align: center;">  <p>Upper surface: 1000 N</p> <p>Bottom surface: Fix</p> <p>Static analysis</p> </div> <div style="text-align: center;"> <p>Nodes: 10141 Elements: 6664</p> </div> <div style="text-align: center;">  <p>Bottom surface: Fix</p> <p>Vibration analysis (Free vibration)</p> </div> </div>	
The calculated properties	Density: 4183 $\text{kg/m}^3$
	Young's modulus: 79.3 GPa

	Specifications of the block	
	Size	60mm×45mm×75mm
	Coarse aggregate	Aluminum (121500 mm <sup>3</sup> , 328 g)
	Middle aggregate	Zinc (48600 mm <sup>3</sup> , 347 g)
	Fine aggregate	Steel (20250 mm <sup>3</sup> , 159 g)
	Bond	Epoxy resin (12150 mm <sup>3</sup> , 14.6 g)
	When the load on upper surface of the block is 1000 N, the displacement in the height direction become -3.3 μm, and the resonance frequencies of the first and the second models are 5208 Hz and 6100 Hz respectively.	

Note: Volume mm<sup>3</sup>, weight g.

Figure 6: Photograph of the new composite material using the material optimization technology and its specifications.

frequencies were thought to be 5200 Hz and 6100 Hz respectively. The necessary properties for achieving the desired characteristics of the block were firstly calculated by the algorithm of the material optimization using inverse analysis of the FEM. The FEMs simulations used were a static and a free vibration analyses. Here, the necessary properties for achieving the desired characteristics of the block were the Young's modulus and density, which were simultaneously considered.

Then the several component materials and the weight percentages for the new composite material with the desired properties were calculated by the developed original software. The calculated results are shown in Table 3. The coarse, middle, fine aggregates and bonding material are aluminum, zinc, steel and epoxy resin, respectively. The weight percentages (volume percentages) were 38.7% (60 vl.%), 40.9% (24 vl.%), 18.7% (10 vl.%) and 1.7% (6 vl.%) respectively. The characteristics, behavior and the properties of the manufactured blocks with the new composite material were experimentally measured and the results are shown in Table 4. For this the following was considered, when the load on the upper surface of the block is 1000 N, the displacement in the height direction was measured by using a

Table 3: The calculated three aggregates and one bond for the new composite material with the optimized properties and these weight percentages.

Components	Aggregates			Bond
Classification	Coarse	Middle	Fine	
Size	φ 10 mm	φ 1.0 mm	φ 0.1 mm	—
Material	Aluminium	Zinc	Steel	Epoxy resin
Density	2700 kg/m <sup>3</sup>	7130 kg/m <sup>3</sup>	7830 kg/m <sup>3</sup>	1200 kg/m <sup>3</sup>
Young's modulus	69 GPa	96.5 GPa	205 GPa	2.6 GPa
Weight (weight %)	328 g (38.7%)	347 g (40.9%)	159 g (18.7%)	14.6 g (1.7%)
Volume (volume %)	121,500 mm <sup>3</sup> (60%)	48,600 mm <sup>3</sup> (24%)	20,250 mm <sup>3</sup> (10%)	12,150 mm <sup>3</sup> (6%)

Note: The block is with length 60 mm×width 45 mm×height 75 mm.





Table 4: Evaluation: the characteristics, behaviour and the properties in the manufactured block with the new composite material.

Desired characteristics	Experimental values	Error※
The displacement: -3.2 $\mu\text{m}$ at 1000 N	-3.5 $\mu\text{m}$	9.4%
The first resonance frequencies: 5200 Hz	5130 Hz	1.3%
The first resonance frequencies: 6120 Hz	6053 Hz	1.3%

Note: Error =  $| \text{Experimental values} - \text{Desired characteristic} | \div | \text{Desired characteristic} | \times 100$ .

compression tester, and the Young's modulus was calculated by using this data. Additionally, the resonance frequencies of the first and the second models of the manufactured block were measured by the frequency response method using an impact hammer, an acceleration pick-up and a FFT. Here, it can be said that the manufactured block has the desired characteristics demanded initially and valuable as an innovation source. This technology was deemed as effective for the design and manufacture of innovative products.

## 7 CONCLUSION

It is concluded from the results that:

- (1) As presented before, the expanded proposed software was able to calculate Young's modulus, density, coefficient of linear expansion, specific heat and thermal conductivity for several properties.
- (2) The material optimization technology was effective for the development of innovative products with defined desired functions or properties. This was achieved through a vertical integration of the previously developed material optimization software, the previously explored manufacturing process and the FEM inverse analysis tools suggested in this research.

## REFERENCES

- [1] Moriwaki, T., Shamoto, E. & Tokunaga, T., Thermal deformation of an ultra-precision machine tool due to environmental temperature change. *Transactions of the Japan Society of Mechanical Engineers, Series C*, **63**(615), pp. 4025–4030, 1997. (In Japanese.)
- [2] Nakajima, H., Lotus-type porous metals. *Bulletin of The Iron and Steel Institute of Japan*, **6**(9), pp. 701–707, 2001. (In Japanese.)
- [3] Kobayashi, T., Matsubayashi, T. & Shibata, K., On the improvement of the damping capacity of a steel structure by overlaying with fiber-reinforced plastics. *Transactions of the Japan Society of Mechanical Engineers, Series C*, **58**(554), pp. 3096–3101, 1992. (In Japanese.)
- [4] Okada, M., Hosokawa, A., Asakawa, N., Fujita, Y. & Ueda, T., Influence of minimum quantity lubrication on tool temperature in end milling of difficult-to-cut materials having low thermal conductivity. *Transactions of the Japan Society of Mechanical Engineers, Series C*, **78**(792), pp. 3093–3103, 2012. (In Japanese.)
- [5] Tanabe, I., Development of technology for creating composite materials of machine tool. *Int. J. of Automation Technology*, **9**(6), pp. 714–719, 2015.
- [6] Russell, H.W., Principles of heat flow in porous insulators. *J. Am. Ceram. Society*, **18**, pp. 1–5, 1956.



- [7] Tanabe, I., Takada, K. & Nakamura, A., Thermal and mechanical characteristics of epoxy resin concrete used in machine tool structures. *Transactions of the Japan Society of Mechanical Engineers, Series C*, **56**(525), pp. 1314–1321, 1990. (In Japanese.)
- [8] Tanabe, I., Mizutani, J. & Yamada, Y., Development of ceramic resin concrete for precision machine tool structures (development of three-dimensional and functionally gradient material). *Transactions of the Japan Society of Mechanical Engineers, Series C*, **62**(596), pp. 1619–1625, 1996. (In Japanese.)
- [9] Tanabe, I., Takiguchi, S. & Iyama, T., Development of software for creating new materials with hybrid properties. *Transactions of the Japan Society of Mechanical Engineers, Series C*, **78**(786), pp. 595–604, 2012. (In Japanese.)
- [10] Tanabe, I., Takada, K. & Nakamura, A., Thermal and mechanical characteristics of epoxy resin concrete used in machine tool structures. *Transactions of the Japan Society of Mechanical Engineers*, **56**(525), pp. 1314–1321, 1990. (In Japanese.)
- [11] Tanabe, I., Mizutani, J. & Yamada, Y., Development of ceramic resin concrete for precision machine tool structures (development of three-dimensional and functionally gradient material). *Transactions of the Japan Society of Mechanical Engineers*, **62**(596), pp. 1619–1625, 1996. (In Japanese.)
- [12] Tanabe, I., Konndo, T., Yamada, Y. & Mizutani, J., Development of three-dimensional and functionally gradient material and evaluation of the composite structure lathe using the material. *Transactions of the Japan Society of Mechanical Engineers*, **64**(627), p. 4472, 1998. (In Japanese.)
- [13] Tanabe I., Development of software for the creation of new materials with hybrid properties. *WIT Transactions on Engineering Sciences*, Vol 116, WIT Press: Southampton and Boston, pp. 139–147, 2017.

